Article no. 30

THE CIVIL ENGINEERING JOURNAL 3-2019

EXPERIMENTAL RESEARCH ON SHEAR STRENGTH CHARACTERISTICS OF SOIL-ROCK MIXTURES

Zhijun Zhou, Dandan Han, Wei Yu, Yaqin Dong*

School of Highway, Chang'an University, Xi'an 710064, China; handandan@chd.edu.cn; 1822237854@qq.com

ABSTRACT

The shear strength of soil-rock mixtures (S-RM) is an important parameter affecting the stability of engineering. Therefore, taking the S-RM along Shiyan-Tianshui Expressway (G7011) in Qinba Mountains as the research object, large-scale direct shear tests on S-RM with different rock content and water content were conducted in this paper. The test results show that the shear deformation curves of S-RM samples are basically the same, which can be divided into four stages: elastic deformation, initial yield, strain hardening and shear failure stages. The cohesion of S-RM decreases with the increase of rock content, and the internal friction angle increases linearly with the increase of rock content. The cohesion increases first and then decrease with the increase of water content, while the internal friction angle and shear strength decrease with the increase of rock content. Then, according to the large-scale direct shear test results, the fitting equations of shear strength and shear strength index of S-RM were obtained, and the fitting equations were verified by an engineering example. The results show that the fitting equations were suitable for loess and gravel mixtures with similar properties, and have important guiding significance for the calculation of shear strength of similar engineering materials.

KEYWORDS

Soil-rock mixture (S-RM), Large-scale direct shear test, Shear strength, Rock content, Water content, Fitting equation

INTRODUCTION

S-RM is an extremely inhomogeneous and loose rock-soil medium system formed since Quaternary, which is composed of high-strength block, fine-grained soil and pore with a certain rock content [1-3]. S-RM is very common in mountainous areas and is widely used as a filler in highway, railway, water conservancy and other engineering construction [4-6]. There are obvious differences in particle size and material composition between the block rock and soil, which constitute S-RM. The traditional geomechanical theory system based on the continuum mechanics theory, which is difficult to describe the mechanical behaviour of the S-RM and the traditional geotechnical test methods are also facing challenges because of soil's complex physical and mechanical properties [7-12]. With the continuous development of engineering construction, more and more engineering problems are closely related to the properties of S-RM. The study of the properties of S-RM has become an urgent problem that should be solved in today's engineering construction, and this study is also the necessity of the development of geomechanics and engineering geology nowadays. In a word, it is of great significance to analyse the shear strength of S-RM [13-15].

The stability of S-RM mainly depends on its shear strength, so the interaction of various factors affecting the shear strength of S-RM leads to the complexity properties of S-RM [16-18]. At present, the methods of describing and analysing the structural characteristics of S-RM by many global famous scholars can be divided into empirical method, fractal theory-based method, mathematical geology method and digital image processing method [19]. It is difficult to know the particle distribution of S-RM through sieving test, so Xu et al. used digital image processing method to get the proportion and distribution of rock mass. According to the test results, the deformation and fracture mechanism of S-RM is controlled by the proportion of block size. And the shape of shear stress-horizontal displacement curve and vertical displacement-horizontal displacement curve of S-RM samples are different from those of common "soil" and "rock" [20,21].

In recent years, based on stereological method, Medley [22-24] proposed a method to estimate the internal rock content by using the chord length of the block exposed by drilling cores, and analysed the error between the rock content value obtained by this method and the actual value. It is believed that the error depends on the shape, content, arrangement direction and research scale of the block. Zhang et al. carried out two large-scale compaction tests and a series of field direct shear tests on soils and S-RM samples. It was found that the mixing of soil and rock made it difficult to determine the mechanical behaviour of S-RM [25]. And various researchers have carried out a series of experiments to study the complex mechanical behaviour of S-RM. Wei et al. carried out large-scale direct shear tests of S-RM because of its complex mechanical behaviour. It was found that the test results are related to the rock content of weathered basalt. When the rock content is different, there is a power law relationship between stress ratio and displacement increment. The horizontal stress is concentrated on the volume strain of rock mass [26]. Based on large-scale direct shear test in laboratory, Zhao et al. studied the influence of rock content, water content, particle size distribution and compactness on the shear strength of S-RM filled with red clay and gravel soil by controlling the mass and volume of the sample to reach the required compactness level. It can be concluded that the order of the above factors affecting the shear strength of S-RM is rock content, water content, degree of compaction, non-uniformity coefficient and coefficient of curvature [27].

Another common problem of S-RM compared with fine-grained soil is the particle size effect in strength analysis. Therefore, by considering the size effect of rock, Ren et al. proposed a systematic method to get the actual shear strength of S-RM. Based on fractal theory, the rock particle size was determined to be 5 mm. On this basis, the effects of engineering size, shear gap effect and sample size on the shear strength of S-RM were studied. The results show that the physical mechanism of S-RM shear resistance based on the change of apparent cohesion and internal friction angle of particles is decided by the clearance of direct shear test [28]. In general, the mechanical behaviour of S-RM mainly depends on the deformation rate, water content and particle size. Therefore, Wei et al. studied the effect of these factors on the mechanical properties of S-RM through a series of large direct shear tests. It was found that the shear rate is faster, the lower strength of macro. And under unsaturated conditions, the strength of rock block decreases due to water content, which affects the strength of S-RM. [29].

Therefore, on the basis of previous studies, this paper specially focuses on the shear strength characteristics of S-RM. In the experimental study, the effects of such factors as the rock content, water content and other factors were considered. According to the test data, the fitting equations of shear strength and shear strength index of S-RM were established, which have certain effect on calculation of shear strength of S-RM.

STUDY AREA

The G7011 is an important highway in Qinba Mountains which links Hubei, Shanxi and Gansu Provinces. Its specific geographic location and structure are shown in Figure 1. During the long-term geological evolution in this area, the metamorphic rock series with obvious anisotropy were basically constructed owing to metamorphic transformation and structural deformation.

The diameter of particles along G7011 ranges from less than 1 mm to more than 5 m, resulting in a large size effect. In addition, the S-RM in this area is mainly composed of Quaternary alluvium and residual slope stratum, which is covered with silty clay-soil, breccia and gravel. According to geological data, the soil-rock mixed slopes in Qinba Mountains (Shaanxi, China) are widely distributed, which seriously affects the safety of the infrastructure and has potential threat to human life and property.

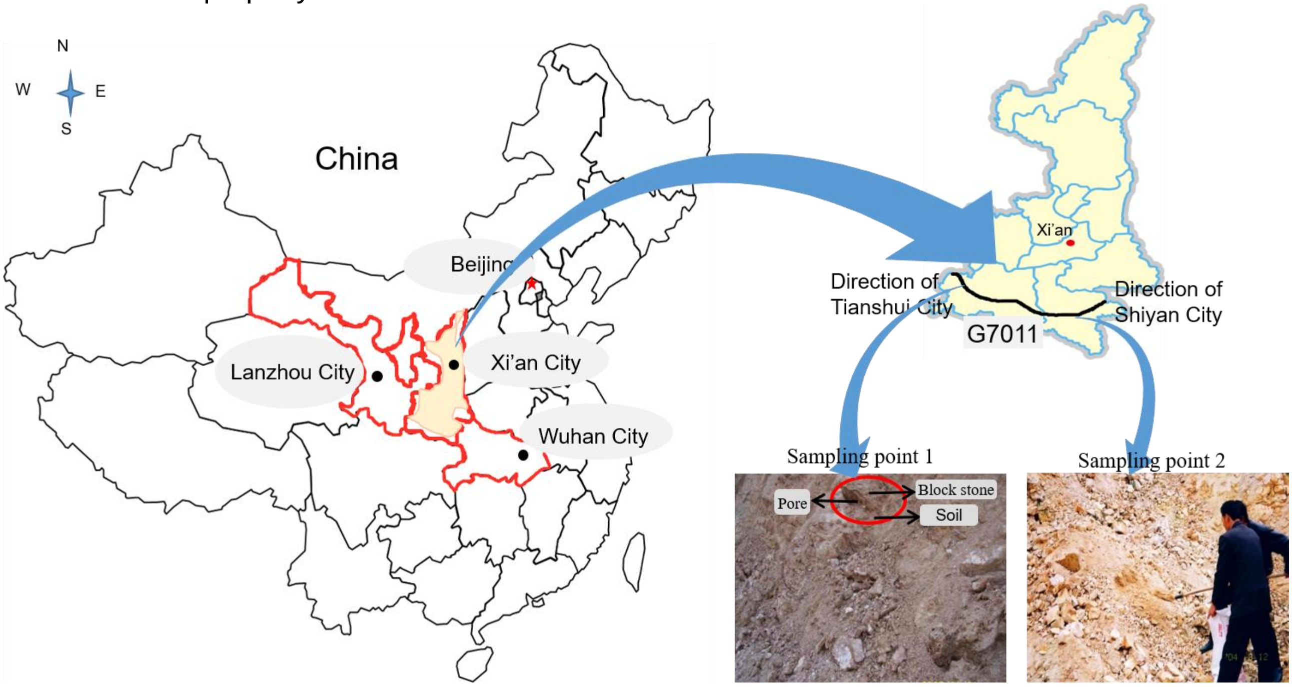

Fig. 1- Geographical location and structural of G7011 (map data © 2018 Baidu maps)

METHODS

Test material

A representative slope along G7011 (K0+140~K0+830) was sampled and defined as sampling point 1. The maximum dry density of S-RM with different rock content were obtained by compaction test, as shown in Table 1.

Tab. 1 - Compaction test results of S-RM with different rock content

Rock content（%）	10	20	30	40	50
maximum dry density (g/cm3)	2.08	2.092	2.11	2.132	2.161

Preparation of Model Samples

In this paper, the size of the sample is less than 60 mm, and the screening test results are shown in Table 2. According to the definition of earth-rock threshold [30], when L_c is 40 cm, the threshold $d_{S/RT}$ of earth-rock limit is 2 cm. Then, according to the principle of similar gradation, the samples were produced according to the rock content of 10%, 20%, 30%, 40% and 50%, respectively. The calculation results of model material gradation test curve are shown in Table 3, and the gradation curves are shown in Figure 2. For S-RM with particle sizes over 60 mm, the equivalent mass of rock with particle sizes of 60 mm is approximately used to instead.

Tab. 2 - Screening test results of model material

Sieve size (mm)	60	40	20	10	5	2	0.5	0.075
Pass Percentage (%)	100	89.1	65.3	54.2	44.8	33.5	14.3	1.9

Tab. 3 - Summary of screening conversion results under different rock contents

Rock content (%)	1/Mr*	Conversion of sieve hole size (mm)							
50	0.375	160	106.7	53.3	26.7	13.3	5.3	1.3	0.2
40	0.75	80	53.3	26.7	13.3	6.7	2.7	0.7	0.1
30	1.2	50	33.3	16.7	8.3	4.2	1.7	0.4	0. 1
20	1.6	37.5	25.0	12.5	6.3	3.1	1.3	0.3	0.0
10	2.1	28.6	19.0	9.5	4.8	2.4	1.0	0.2	0.0
Pass Percentage (%)		100	89.1	65.3	54.2	44.8	33.5	14.3	1.9

Note: *Mr means similar gradation module ratio

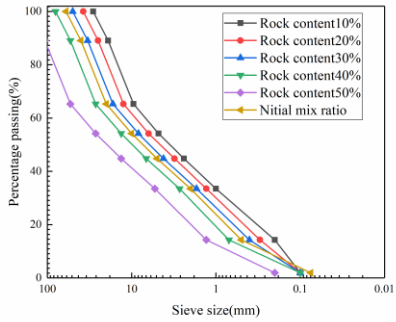

Fig. 2 - Gradation curves with different rock contents

To find the influence of rock content and water content on the shear strength of S-RM. The samples were prepared with different rock content (10%, 20%, 30%, 40%, 50%) and water content (0%, 5%, 10%, 15%) respectively. And there were 20 groups of samples with 3 samples in each group. The specific parameters of the sample are shown in Table 4.

Tab. 4 - Test conditions and direct shear test results of sample point 1

Water content (%)	Index name	Rock content (%)				
		10	20	30	40	50
0	c (kPa)	14.52	13.37	10.44	5.91	3.3
	φ (°)	25.95	28.34	30.61	32.91	35.48
5	c (kPa)	15.36	14.22	11.29	6.76	4.15
	φ (°)	24.04	26.43	28.7	31	33.57
10	c (kPa)	14.74	13.6	10.66	6.13	3.52
	φ (°)	21.99	24.38	26.65	28.95	31.52
15	c (kPa)	12.64	11.5	8.57	4.04	1.43
	φ (°)	19.81	22.19	24.47	26.76	29.33

Test methods and procedures

As shown in Figure 3, the sample size of the large direct shear apparatus used in the test was 500 mm x 500 mm x 400 mm. During the test, the upper shear box was controlled to be fixed, and a certain horizontal shear force was applied to the lower shear box to make the lower shear box displace and complete the shear of the sample.

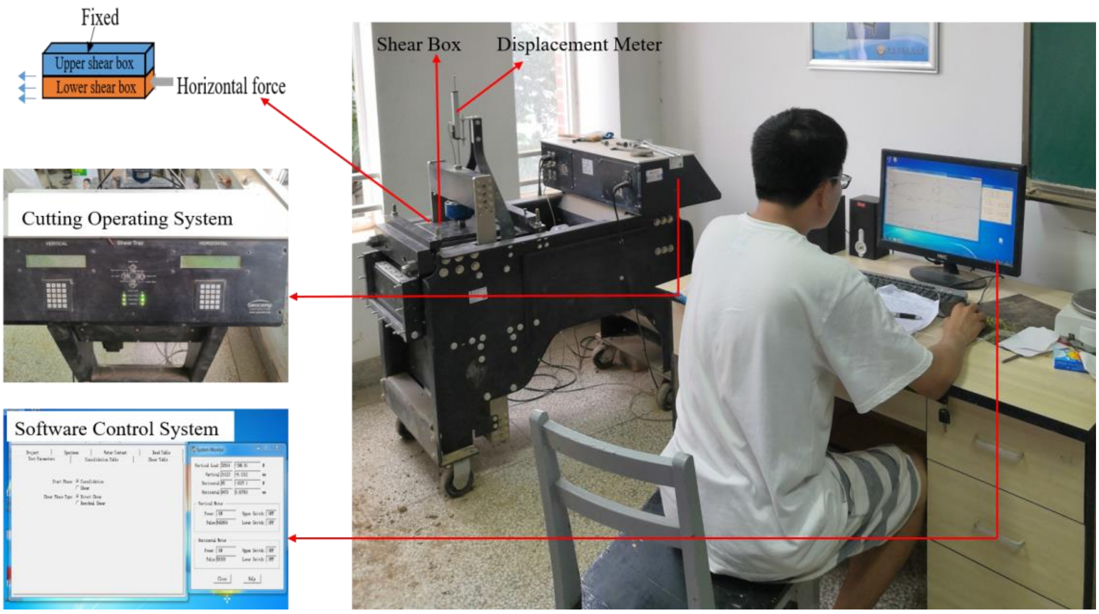

Fig. 3 - Schematic diagram of the large direct shear apparatus

The test process is as follows and sample preparation process is shown in Figure 4.

(1) According to the requirements of test conditions and gradation curve mentioned above, the proper S-RM samples were made. The mixture is evenly mixed and the stuffy material is kept for 24 hours.

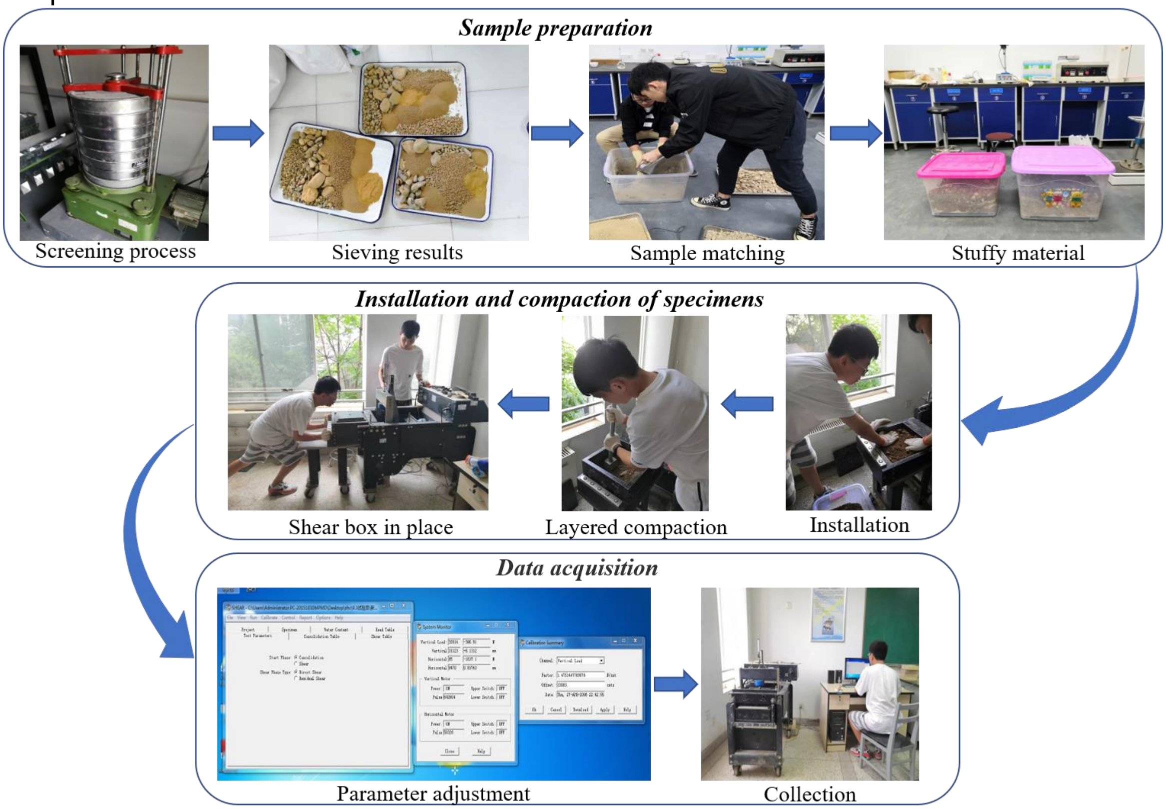

Fig. 4 - Operation process of large direct shear test

DOI 10.14311/CEJ.2019.03.0030

(2) The S-RM samples were packed into a shear box in three layers and compacted by layers. Then, they were compacted and scratched by applying vertical pressure step by step. The direct shear test was carried out after the deformation was stable, and the consolidation rate was set to 1 mm/min.

(3) Set the horizontal shear speed of direct shear apparatus to 1.4 mm/min. When the stable residual shear stress or shear displacement of the shear curve reached 40 mm (8% of the specimen diameter), the shear was stopped, the test data were stored and the specimen was taken out.

(4) Each specimen was subjected to normal stress of 200 kPa, 300 kPa and 400 kPa, respectively.

RESULTS

Based on the large-scale direct shear test results, the shear stress-shear displacement curves under different rock contents are plotted, as shown in Figure 5.

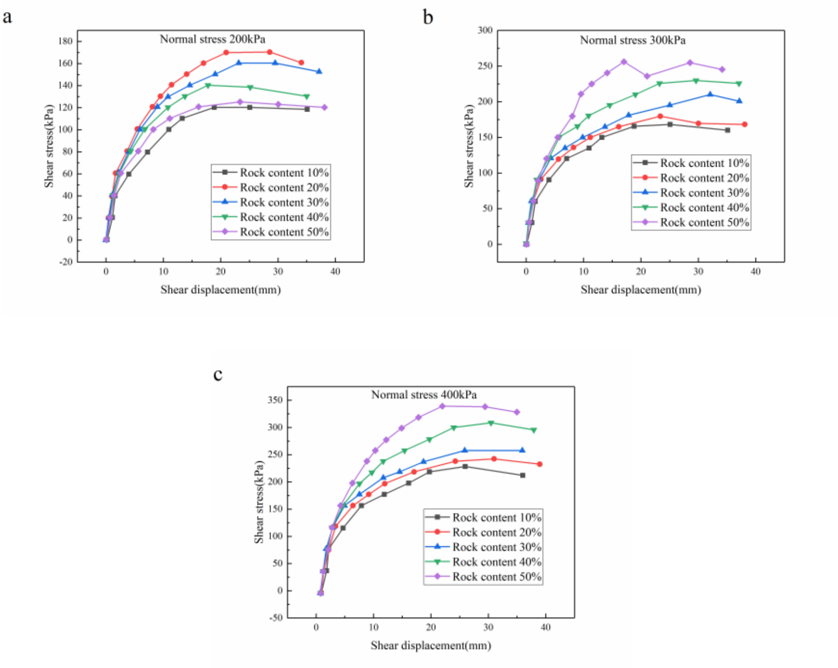

Fig. 5 - Shear stress-shear displacement curves of S-RM specimen

From Figure 5, it can be seen that the shear strength of S-RM increases with the increase of normal stress. Under the same normal stress, the shear strength of S-RM increases with the increase of rock content. The shear deformation curves of S-RM samples are basically the same, which can be divided into elastic deformation, initial yield, strain hardening and shear failure stages [31,32]. When the shear displacement reaches the second half of the initial yield stage (about 18 mm-30 mm), the shear stress of the sample will increase again until the maximum shear strength is reached due to the interlocking of rocks. In the process of increasing shear displacement, the rock moves and rotates continuously under the action of occlusion force, which makes the arrangement of rock adjust continuously, resulting in the decrease of shear stress of the specimen.

Analysis of Influencing Factors

Effect of rock content on shear strength

According to Table 4, the experimental curves of rock content, cohesion and internal friction angle of the S-RM are drawn, as shown in Figure 6. It can be seen from the Figure 6(a) that when the rock content is less than 20%, the influence of rock content on cohesion is relatively small; When the rock content is between 20% and 40%, the cohesion is greatly affected by the rock content. During shearing, with the increase of rock content, the contact and biting between blocks in S-RM may also increase (Figure 7), resulting in an increase in cohesion. But with the increase of rock content, the content of fine particles decreases, accompanied by the decrease of cohesion between fine particles. When the decrease of cohesion caused by the decrease of fine particles is greater than increase caused by biting, the cohesion generally shows a downward trend.

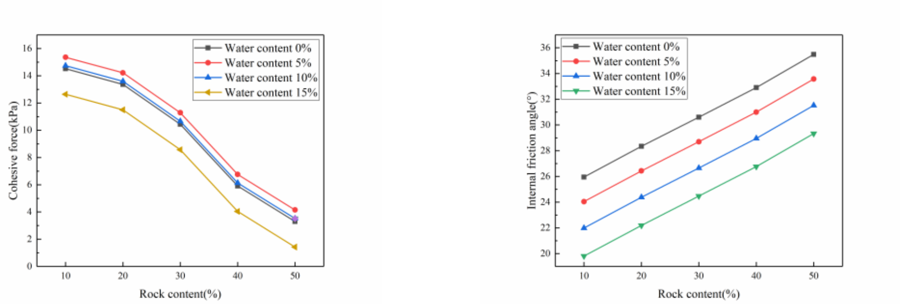

(a) Cohesion force-rock content curves; (b) Internal friction angle-rock content curves

Fig. 6 - Shear strength index-rock content curves of specimens with different water contents

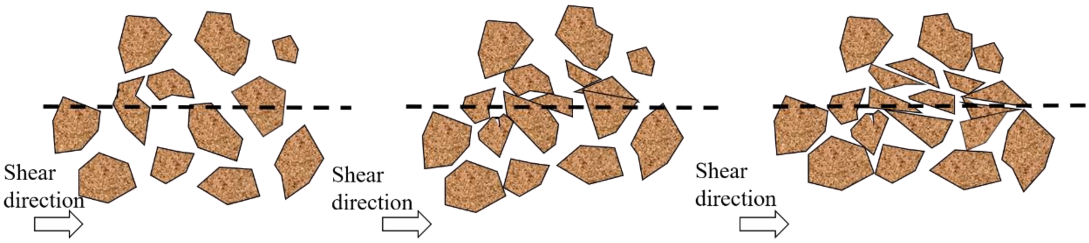

(a) Stage 1 (b) Stage 2 (c) Stage 3

Fig. 7 - Sketch of shear surface and internal rock movement of S-RM (The dashed line is the shear surface)

It can be seen from the Figure 6(b) that the internal friction angle increases linearly with the increase of rock content. This is because that with the increase of rock content, the skeleton of S-RM gradually forms, and the intercalation between particles increases [33]. Referring to the previous research results [27,34-36], the following equation can be obtained:

$$\varphi_{p_2}=0.238p_2+23.57 \quad (10<p_2<50) \qquad (1)$$

Where φ_{p_2} (°) is the internal friction angle of the S-RM with the rock content of p_2, and p_2 (%) is the rock content.

The reasons for the above test results can also be explained by the composition of S-RM. For fine-grained soil, its strength is mainly embodied by cohesion; for gravel, its strength is mainly embodied by internal friction angle. Therefore, with the increase of rock content and the decrease of fine-grained soil, the internal friction angle increases and the cohesion decreases. That is to say, the S-RM changes from "soil" to "rock".

Effect of water content on shear strength

It can be seen from Figure 8 that the shear strength increases with the increase of normal stress, but the shear strength of S-RM decreases with the increase of water content due to the softening of soil when it meets water. This is consistent with the rule of the influence of water content of fine grains on shear strength [21].

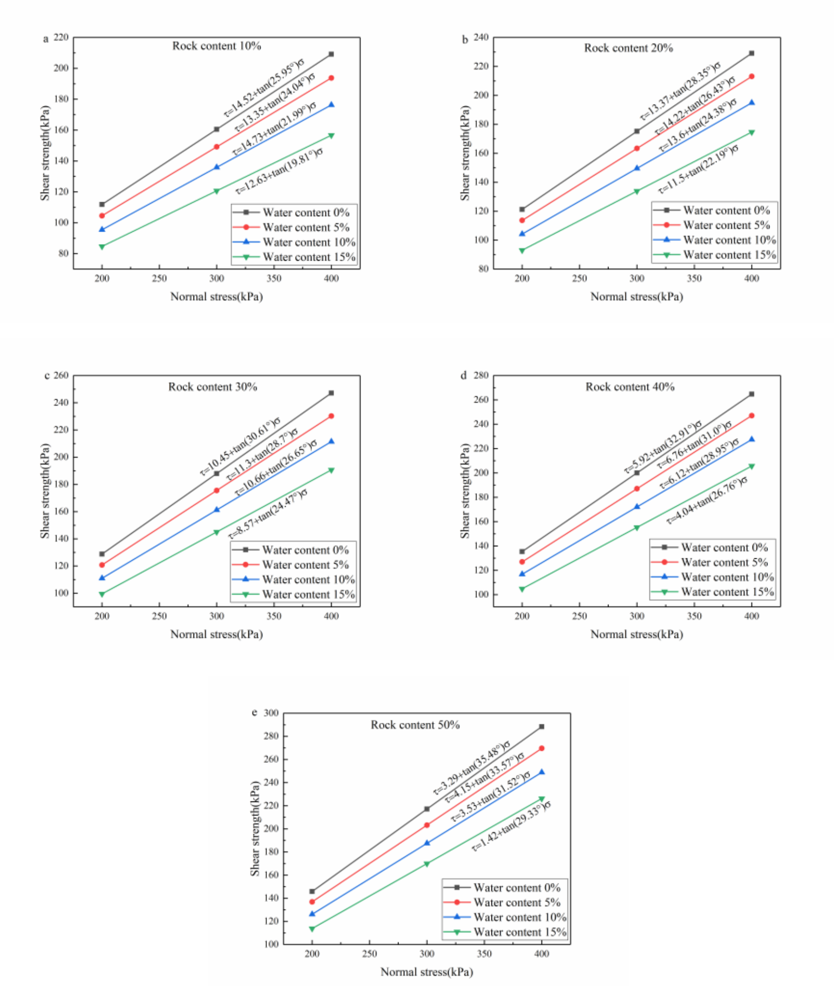

Fig. 8 - Shear strength-normal stress curves of specimens with different water contents

According to Table 4, the experimental curves of water content, cohesion force and internal friction angle of S-RM are drawn, as shown in Figure 8. From Figure 9(a), we can found that the cohesion force of S-RM increases first and then decreases with the increasing water content. This is because when the water content is small, the increase of water content will form a combined water film, which can make the particles directly shear and compact. However, when the water content is too high, the intrinsic attraction between the particles will gradually weaken, so the cohesion increases first and then decreases.

From Figure 9(b), the internal friction angle decreases linearly with the increase of water content. On the one hand, due to the increase of water content, the soil particles become very soft, and the mud adhering to the surface of coarse grains plays a lubricating role, which reduces the friction resistance between the particles, thus reducing the internal friction angle. On the other hand, due to the increase of water content, some hard coarse grains are softened, which indirectly reduces the content of coarse grains, thus causing the reduction of internal friction angle.

DOI 10.14311/CEJ.2019.03.0030

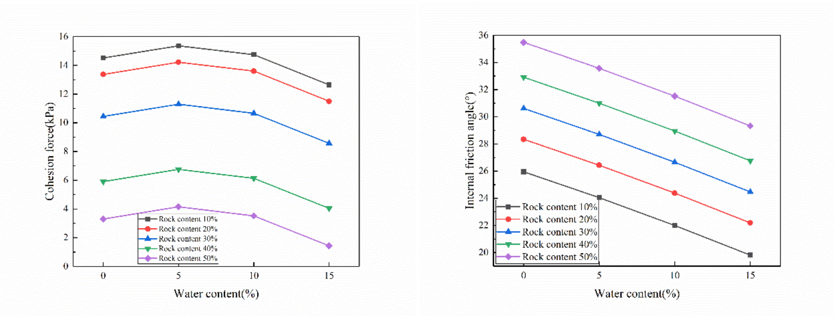

(a) Cohesion force-water content curves; (b) Internal friction angle-water content curves

Fig. 9 - Shear strength index- water content curves of specimens with different rock contents

Shear Strength Fitting

In practical engineering, the stability of S-RM is controlled by their shear strength. In order to obtain the relationship between shear strength of S-RM and rock content, water content and normal stress, the shear strength of S-RM is regressively analysed, and the fitting equations of S-RM are obtained. As shown below：

$$\begin{aligned} &Y = Ap_2^{\ 2} + Bw^2 + C\sigma^2 + Dp_2 + Ew + F\sigma + Gp_2 w^2 + Hp_2\sigma^2 + \\ &Iw\sigma^2 + Jp_2 w + Kp_2\sigma + Lw\sigma + M \\ &A = 0.0022, B = -0.03924, C = -3.17501\times10^{-7}, D = -0.33806, \\ &E = 0.824221, F = 0.43758, G = 5.7\times10^{-5}, H = 1.125\times10^{-8}, \\ &I = -1.6\times10^{-6}, J = -0.01293, K = 0.00529, L = -0.00917, \\ &M = 17.0.2913 \end{aligned} \tag{2}$$

$$c = -0.00324p_2^{\ 2} - 0.02943w^2 + 6\times10^{-6}p_2 w - 0.10472p_2 + 0.31628w + 16.21115 \tag{3}$$

$$\varphi = 2.78571\times10^{-4}p_2^{\ 2} - 0.00276w^2 - 1.2\times10^{-5}p_2 w + 0.21963p_2 - 0.368w + 23.763 \tag{4}$$

Where p_2 is the rock content, w is the water content, σ is the normal stress, Y is the shear strength, c and φ are the cohesive force and the internal friction angle, respectively.

From Figures 10-12, it can be seen that the shear strength curves calculated by the fitting equation (2) are all in good agreement with the measured value, and the correlation index R^2 of the shear strength curve is 0.99945. Figure 13 are the fitting curves and measured value of shear strength index. The correlation index R^2 of equation (3) is 0.977864, and the correlation index R^2 of equation (4) is 0.99975.

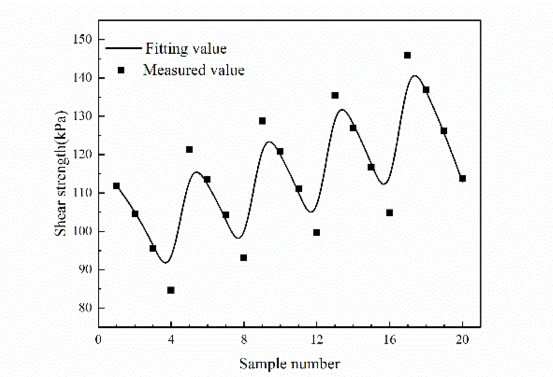

Fig. 10 – Moment fitting curves of shear strength (σ =200kPa)

DOI 10.14311/CEJ.2019.03.0030

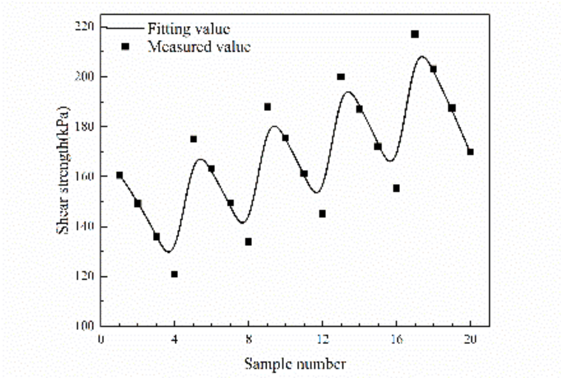

Fig. 11 – Moment fitting curves of shear strength (σ =300kPa)

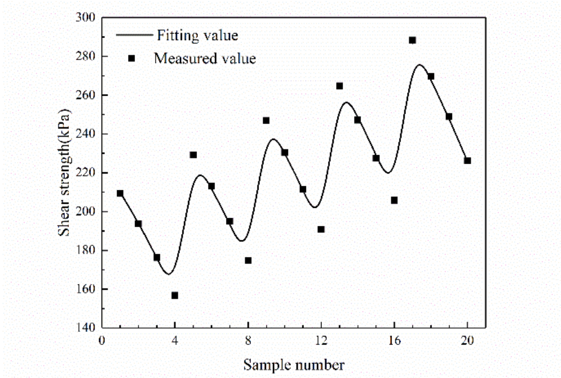

Fig. 12 – Moment fitting curves of shear strength (σ =400kPa)

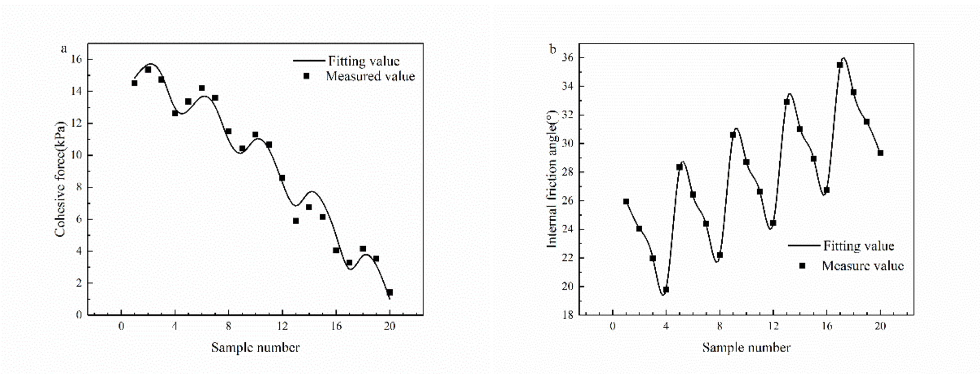

Fig. 13 – Moment fitting curves of shear strength index

Verification of fitting equation

In order to verify the applicability of the above fitting *equations*, we sampled another representative slope along the *G7011* (K4+410~K4+640) and defined it as sampling point 2. Large-scale direct shear tests were conducted with soil samples from sampling point 2 to obtain the shear strength index values under different operating conditions, as shown in Table 5.

Tab. 5 - Test conditions and direct shear test results of sampling point 2

Water content (%)	Index name	Rock content (%)				
		10	20	30	40	50
1	c (kPa)	14.94	12.98	10.76	7.33	3.31
	φ (°)	25.76	28.26	30.31	33.41	34.65
4	c (kPa)	15.59	13.71	11.45	7.91	3.74
	φ (°)	24.71	26.73	29.42	31.51	34.02
8	c (kPa)	15.38	13.32	10.69	7.52	3.47
	φ (°)	22.76	24.97	27.41	30.10	32.41
12.5	c (kPa)	14.12	12.23	9.53	6.04	2.33
	φ (°)	20.54	23.62	25.49	27.82	30.53

In order to verify whether the two sets of data in Table 4 and Table 5 are suitable for the same fitting equation, the data in Table 5 were fitted with the same functions as those in equations (3) and (4) in origin 2017. The number of data points, degree of freedom and sum of squares of residuals in the fitting report were used in the process of comparison. After that, the two sets of data are compared and the result report was generated, mainly by F-test. The confidence probability in the item indicates that the confidence probability of the formula of cohesion and internal friction angle approaches 0 in the result report (Figure 14), which indicates that the two sets of data are suitable for the current fitting equations respectively.

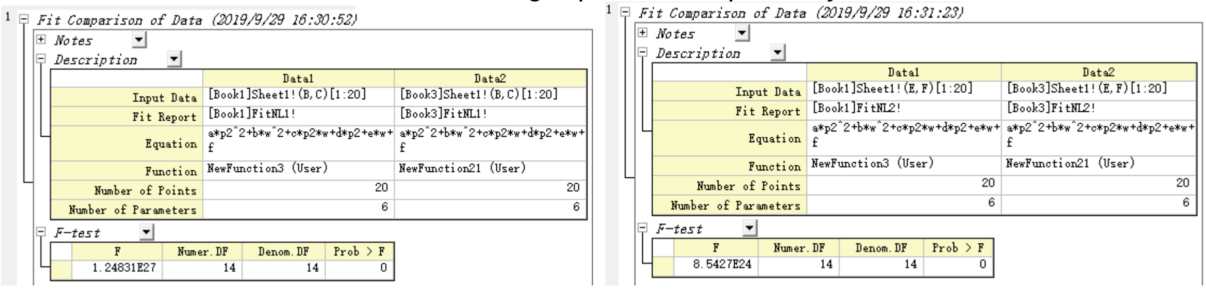

1 Fit Comparison of Data (2019/9/29 16:30:52)

Notes

Description

	Data1	Data2
Input Data	[Book1]Sheet1!(B,C)[1:20]	[Book3]Sheet1!(B,C)[1:20]
Fit Report	[Book1]FitNL1!	[Book3]FitNL1!
Equation	a*p2^2+b*w^2+c*p2*w+d*p2+e*w+f	a*p2^2+b*w^2+c*p2*w+d*p2+e*w+f
Function	NewFunction3 (User)	NewFunction21 (User)
Number of Points	20	20
Number of Parameters	6	6

F-test

F	Numer.DF	Denom.DF	Prob > F
1.24831E27	14	14	0

1 Fit Comparison of Data (2019/9/29 16:31:23)

Notes

Description

	Data1	Data2
Input Data	[Book1]Sheet1!(E,F)[1:20]	[Book3]Sheet1!(E,F)[1:20]
Fit Report	[Book1]FitNL2!	[Book3]FitNL2!
Equation	a*p2^2+b*w^2+c*p2*w+d*p2+e*w+f	a*p2^2+b*w^2+c*p2*w+d*p2+e*w+f
Function	NewFunction3 (User)	NewFunction21 (User)
Number of Points	20	20
Number of Parameters	6	6

F-test

F	Numer.DF	Denom.DF	Prob > F
8.5427E24	14	14	0

(a)Cohesion Result Statement; (b) Report of results of internal friction angle

Fig. 14 – Result Report of Data Set Comparisons

According to the above large-scale direct shear tests, equations (3) and (4) were selected to calculate the shear strength index of the S-RM at sampling point 2 under different rock content and water content, and the theoretical calculation values were compared with the large-scale direct shear test results of the S-RM at sampling point 2, as shown in Figure 15.

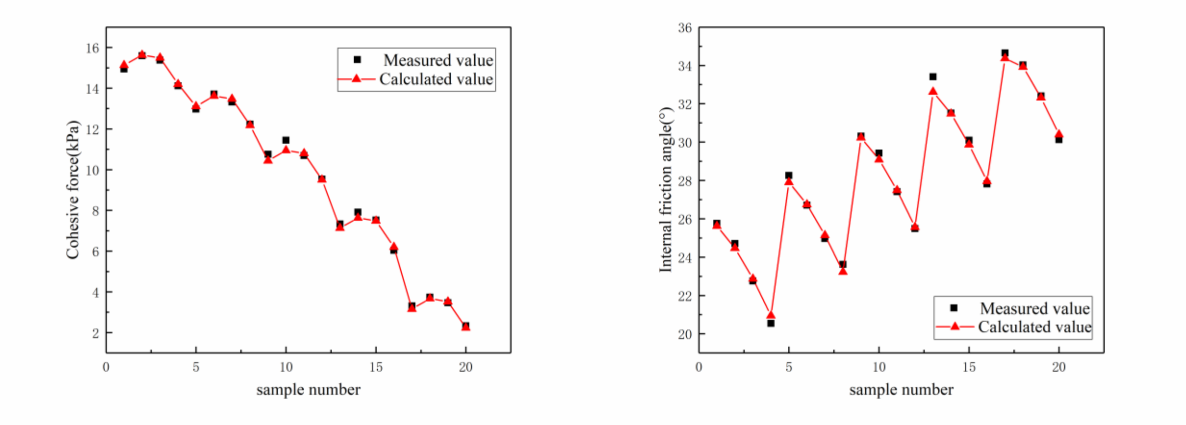

(a) Cohesion comparison; (b) Comparison of internal friction angles

Fig. 15 – Comparison of calculated and measured values

DOI 10.14311/CEJ.2019.03.0030

By comparing the relative errors between the measured and calculated values of sampling point 2 under different working conditions, as shown in Table 6. From the error statistics, it can be seen that the relative error of cohesion is less than 5%. The relative error of 50% rock content and 1% water content is the biggest, which is 4.75%, while that of 30% rock content and 12.5% water content is the smallest, which is 0.21%. The relative error of internal friction angle is less than 3%. The relative error is the largest when the rock content is 40% and the water content is 1%, which is 2.42%. The relative error is the smallest when the rock content is 20% and the water content is 4%, which is 0.15%.

Tab. 6 - Error statistics

	Cohesion					Internal friction angle				
Working Condition	1	2	3	4	5	1	2	3	4	5
Relative error(%)	1.26	0.26	0.71	0.56	0.99	0.55	0.98	0.48	1.96	1.29
Working Condition	6	7	8	9	10	6	7	8	9	10
Relative error(%)	0.66	1.11	0.41	3.07	4.57	0.15	0.68	1.68	0.26	1.13
Working Condition	11	12	13	14	15	11	12	13	14	15
Relative error(%)	1.02	0.21	2.81	3.67	0.40	0.29	0.31	2.42	0.10	0.77
Working Condition	16	17	18	19	20	16	17	18	19	20
Relative error(%)	2.58	4.75	1.91	1.42	4.48	0.50	0.81	0.29	0.28	0.89

In conclusion, we can draw a conclusion that the equations (3) and (4) have certain applicability and can be applied to the mixture of loess and gravel with similar properties. When the rock content is less than 50% and the water content is less than 15%, the shear strength parameters under different rock content can be deduced by measuring the water content of fine soil in the S-RM according to the conventional test, so as to be used by engineers and technicians.

CONCLUSIONS

In this paper, based on large-scale direct shear test, the influence of rock content and water content on shear strength of S-RM was studied. Based on the analysis of the test results, the following conclusions are drawn:

(1) According to the test results, it was found that the shape of shear deformation curve of S-RM is basically the same. It can be divided into elastic deformation, initial yield, strain hardening and shear failure stages. When the shear displacement reaches the second half of the initial yield stage (about 18 mm-30 mm), the shear stress of the sample will increase again until the maximum shear strength is reached due to the interlocking of rocks. In the process of increasing shear displacement, the rock moves and rotates continuously under the action of occlusion force, which makes the arrangement of rock adjust continuously, resulting in the decrease of shear stress of the specimen.

(2) The cohesion force of S-RM decreases with the increasing rock content. When the rock content ranges from 20% to 40%, the influence coefficient of cohesion force is greatly affected by rock content, which is basically 0.373. The internal friction angle increases linearly with the increase of rock content.

(3) The cohesion force of S-RM increases first and then decreases with the increase of water content; the internal friction angle and shear strength decrease with the increase of water content.

(4) Through the non-linear regression analysis of shear strength, the fitting equation of shear strength of S-RM is obtained. And the correlation index R^2 is 0.99945. The correlation index of fitting equation of shear strength index R^2 is 0.97864 and 0.99975, respectively. The next step is to modify the fitting equation through more indoor and actual engineering field test data, so as to facilitate the reference of similar engineering materials design.

CONFLICTS OF INTEREST

The author declares that there is no conflict of interest in this paper.

ACKNOWLEDGEMENTS

A short section may acknowledge special assistance and sources of research This study was financially supported by the National Key R&D Program of China (No. 2018YFC0808706).

REFERENCES

[1] W. J. XU, H.Y. ZHANG, 2013. Research status and development trend of earth-rock mixture. Advances in Science and Technology of Water Resources, vol. 33(1): 80–88. (In China)

[2] W. J. XU, 2008. Study on microstructural mechanics of soil-rock mixture and slope stability. Beijing: Institute of Geology and Geophysics, Chinese Academy of Sciences. (In China)

[3] W. J. XU, R. L. HU, 2009. Conception, classification and significations of soil-rock mixture. Hydrogeology Engineering Geology, vol. 2009(4):50-56. (In China)

[4] H. J. CHAI, Q. Y. CHEN, X. C. KONG, Y. DONG, 2004. Summary of research on construction technology of earth-rock mixed filling subgrade, vol. 25(6): 1005-1010. (In China)

[5] J. L. HAN, S. R. WU, D. L. LI, C. X. TAN et al., 2007. Distribution law and cause of geological disasters in Qinba Mountains. Geological Science and Technology Information, vol. 26(1):101-108. (In China)

[6] Y. F. WU, 2012. Study on deformation and failure mechanism of landslide of the soil-rock mixture in the Qinba Mountain [M. A. Thesis]. Chang'an University. (In China)

[7] T. A. MILLER, G. F. SOWERS, 1957. The strength characteristics of soil-aggregate mixtures. Highway Research Board Bulletin, vol. 183: 16-23.

[8] H. KAWAKAMI, H. ABE, 1970. Shear characteristics of saturated gravelly clays. Transactions of the Japanese Society of Civil Engineers, vol. 2(2): 295-298.

[9] J. P. SAVELY, 1990. Determination of shear strength of conglomerates using a caterpillar D9 ripper and comparison with alternative methods. International Journal of Mining and Geological Engineering, vol. 8(3):203-225.

[10] R. J. FRAGASZY, W. SU, F. H. SIDDIQI, 1990. Effects of oversize particles on the density of clean granular soils. Geotechnical Testing Journal, vol. 13(2): 106-114.

[11] R. J. FRAGASZY, W. SU, F. H. SIDDIQI, 1991. Modeling strength of sandy gravel. Journal of Geotechnical and Geoenvironmental Engineering, vol. 118: 920-935.

[12] F. HU, Z. Q. LI, R. L. HU, Y. X. ZHOU, R. Q. YUE, 2018. Research on the deformation characteristics of shear band of soil-rock mixture based on large scale direct shear test. Chinese Journal of Rock Mechanics and Engineering, vol. 37(3): 766-778. (In China)

[13] W.W. GAO, W. GAO, R. L. HU et al., 2018. Microtremor survey and stability analysis of a soil rock mixture landslide: a case study in Baidian town, China. Landslides, vol. 15(10): 1951–1961.

[14] Y. N. DU, P.F. XU, S.Q. LING, 2017. Microtremor survey of soil-rock mixture landslides: An example of Baidian township, Hengyang City. Chinese Journal of Geophysics-Chinese Edition, vol. 61(4): 1596–1604.

[15] X. LI, Q. L. LIAO, J. M. HE, 2004. In situ tests and a stochastic structural model of rock and soil aggregate in the Three Gorges reservoir area, China. International Journal of Rock Mechanics & Mining Sciences, vol. 41(3): 494-494.

[16] K. M. FUTALAN, J. R. D. BISCARO, R. M. SATURAY et al., 2010. Assessment of potential slope failure sites at Mt. Can-abag, Guinsaugon, Philippines, based on stratigraphy and rock strength. Bulletin of Engineering Geology and the Environment, vol. 69(4): 517–521.

[17] B. NICK, 2013. Shear strength criteria for rock, rock joints, rockfill and rock masses: Problems and some Solutions, Journal of Rock Mechanics and Geotechnical Engineering. vol. 5(4): 249–261.

[18] D. CRUDEN , H. X. LAN, 2014. Using the Working Classification of Landslides to Assess the Danger from a Natural Slope. In: Proceedings of the 12th International IAEG Congress, Torino, Italy, Sep 15-19, 3–12.

[19] C. LIU, L. J. SU, W. J. LIU, 2015. Review of Meso-Structure Characteristic of Soil-Rock Mixture in Accumulation Landslides. Mountain Research, vol. 33(3): 348-355.

[20] W. J. XU, Q. XU, R. L. HU, 2011. Study on the shear strength of soil–rock mixture by large scale direct shear test. International Journal of Rock Mechanics & Mining Sciences, vol. 48 (2011): 1235–1247.

[21] W. J. XU, R. L. HU, Z. Q. YUE, 2008. Meso-structure character of soil-rock mixtures based on digital image. Journal of Liaoning Technical University: Natural Science, vol. 27(1): 51-53. (In China)

[22] E. MEDLEY, 1994. Using stereological methods to estimate the volumetric proportions of blocks in mélanges and similar block-in-matrix rocks (bimrocks). In: Proceedings of the 7th Congress of the International Association of Engineering Geology. Rotterdam: Balkema, 1031-1040.

[23] E. MEDLEY, 1997. Uncertainty in estimates of block volumetric proportions in mélange bimrocks. In: Proceedings of the International Symposium on Engineering Geology and the Environment, IAEG. Rotterdam: Balkema, 267-272.

[24] E. MEDLEY, 2002. Estimating block size distributions of mélanges and similar block-in-matrix rocks (Bimrocks). In: Proceedings 5th North America Rock Mehcanics Symposium (NARMS). Toronto: University of Toronto Press, 509-606.

[25] Z. L. ZHANG, W. J. XU, W. XIA, H. Y. ZHANG, 2015. Large-scale in-situ test for mechanical characterization of soil–rock mixture used in an embankment dam. International Journal of Rock Mechanics & Mining Sciences, vol. 86:317-322.

[26] H. Z. WEI, W. J. XU, F. XU, Q. S. MENG, et al., 2018. Mechanical properties of strongly weathered rock–soil mixtures with different rock block contents. International Journal of Geomechanics, vol. 18(5), Article ID 04018026.

[27] M. H. ZHAO, J. J. LIU, H. LUO, M. H. YANG,2017. Experimental studies of shear strength characteristics and influencing factors of soil-rock aggregate mixture. Rock and Soil Mechanics, vol. 38(4): 965-972. (In China)

[28] M. H. REN, G. S. ZHAO, X. H. QIU, Q. H. XUE, M. T. CHEN, 2018. A Systematic Method to Evaluate the Shear Properties of Soil-Rock Mixture considering the Rock Size Effect. Advances in Civil Engineering, vol. 2018, Article ID 6509728.

[29] H. Z. WEI, W. J. XU, C. F. WEI, Q. S. MENG, 2018. Influence of water content and shear rate on the mechanical behavior of soil-rock mixtures. Science China Technological Sciences, vol. 61(8): 1127-1136.

[30] E. MEDLEY, 1994. The engineering characterization of mélanges and similar block-in-matrix rocks (bimrocks) Berkeley: University of California at Berkeley.

[31] W. J. XU, R. L. HU, R. J. TAN, R.Y. ZENG, H.Q. YU, 2006. Study on field test of rock-soil aggregate on Right Bank of Longpan in Tiger-Leaping Gorge Area. Chinese Journal of Rock Mechanics and Engineering, vol. 25(6): 1270-1276. (In China)

[32] H. F. DENG, X. F. YUAN, J. L. LI, Q. LUO, M. ZHU, 2013. Research on failure characteristics and determination method for shear strength of earth-rock aggregate in direct shear tests. Chinese Journal of Rock Mechanics and Engineering, vol. 32(2): 4065-4072. (In China)

[33] W. J. XU, S. WANG, 2016. Meso-mechanics of soil-rock mixture with real shape of rock blocks based on 3D numerical direct shear test. Chinese Journal of Rock Mechanics and Engineering, vol. 35(10): 2152-2160. (In China)

[34] W. M. SHI, H. L. ZHENG, W. P. LIU, Y. R. ZHENG, 2005. Experiment research on shear strength index of gravel-soil in Three-Gorge reservoir area. Chongqing architecture, vol. 2005(2): 30-35. (In China)

[35] E. S. Lindquist, 1994. The strength and deformation properties of mélange [Ph. D. Thesis]. University of California, Berkeley.

[36] E. W. Medley, 1999. Systematic characterization of mélange bimrocks and other chaotic soil/rock mixtures. Felsbau Rock Soil Engin, vol. 17(3):152–62.